J. Fluid Mech. (2009), *vol.* 622, *pp.* 321–344.
doi:10.1017/S0022112008005247 Printed in the United Kingdom

On pressure invariance, wake width and drag prediction of a bluff body in confined flow

W. W. H. YEUNG†

School of Mechanical and Aerospace Engineering,
Nanyang Technological University, Singapore

(Received 14 July 2008 and in revised form 3 November 2008)

In the present investigation, the form drag on a bluff body in confined flow is studied. From the observation of invariance in pressure distribution between a disk and a flat plate normal to free upstream in unconfined flow, a linear relation linking the drag to the base pressure is derived when the potential-flow model by Parkinson & Jandali (*J. Fluid Mech.*, vol. 40, 1970, p. 577) is incorporated. A theoretical wake width deduced from well-documented experimental data for a disk is proposed such that the wake Strouhal number is independent of inclination. This width, when combined with the momentum equation and solved simultaneously with the aforementioned linear equation, leads to realistic predictions of the drag and the base pressure. The method is consistent when applied to a cone of arbitrary vertex angle, a circular cylinder at subcritical Reynolds numbers and a sphere at subcritical as well as supercritical Reynolds numbers. The case of the inclined disk is also discussed. As the pressure distribution is invariant under wall constraint, analytical expressions for the effect of confinement on the loading of bluff bodies are derived and found to provide the correct trend of experimental data.

1. Introduction

The study of bluff-body flows is an important area of fluid dynamics already commanding a vast literature. For example, the similarity of wake flow downstream of two-dimensional bluff bodies has been studied experimentally by Roshko (1954) and Bearman (1967), among others, through intrinsic parameters such as Strouhal number, wake width, base pressure and drag. Based on the velocity at separation and a theoretical wake width from the 'notched hodograph' theory, a universal Strouhal number (about 0.164) was proposed by Roshko (1954). The Kronauer stability criterion of vortex street led Bearman (1967) to devise a new universal wake Strouhal number (about 0.181), which allows a theoretical relationship for Strouhal number, body drag coefficient and base pressure for two-dimensional bluff bodies to be formulated. While the review by Roshko (1993) is on variations of drag and base suction on two-dimensional bluff bodies, the article by Bearman (1998) provides recent advances in bluff-body flows, including a section on the drag reduction by introducing three-dimensionality. As the flow around two-dimensional bluff bodies has received much attention, it is concluded in Roshko (1954) that 'nominally axisymmetric flows . . . deserve more attention from laboratory and numerical experimenters. Finally, we must keep in mind the basic problem, to find suitable models for the forces on bluff bodies'. The present investigation aims to develop along this remark.

† Email address for correspondence: mwhyeung@ntu.edu.sg

The bluff bodies considered in this study include a disk, a cone of arbitrary apex angle, a circular cylinder and a sphere. They are chosen partly because they are canonical and partly because of their numerous practical applications as widely cited in the literature, such as (*i*) turbulence measurements in wind tunnels in Platt (1937), (*ii*) drag reduction on road vehicles in Saunders (1966), (*iii*) nuclear reactors working with spherical fuel elements in Achenbach (1972), (*iv*) parachute design in Roberts (1980), (*v*) wind-tunnel design in Macha, Buffington & Henfling (1991) and Summer & Brundrett (1995), (*vi*) shedder design in flow metres in Miau and Liu (1990), (*vii*) reconfiguration subject to wind loading in Schouveiler & Boudaoud (2006), among others. It is also noted that well-documented experimental data related to these configurations are available for reference. For instance, Calvert (1967*a*, 1967*b*, 1972) measured the Strouhal number of cones of various apex angles, a disk at different inclinations and a sphere over a range of Reynolds numbers, leading to a wake Strouhal number (about 0.19).

There have been many computational models reported in the literature on the flow past the axisymmetric bluff bodies. For a disk, the studies are mainly for the flow at low Reynolds numbers, such as Masliyah & Epstein (1970) for Reynolds numbers up to 100 (see its references for earlier studies). Pitter, Pruppacher & Hamielec (1973) investigated the flow at low and intermediate Reynolds numbers. As for a sphere, Fornberg (1988) calculated the steady flow at Reynolds numbers up to 5000. More recently, Tomboulides & Orszag (2000) investigated numerically the transitional and weak turbulent flow. And, adaptive direct numerical and large-eddy simulations were used by Hoffman (2006) to compute the drag at a Reynolds number of 10^4. A numerical method incorporating some of the ideas from the model by Parkinson & Jandali (1970) was developed by Bearman & Fackrell (1975) and extended to axisymmetric bluff bodies in good agreement with measurements. Suitable reference to Bearman & Fackrell (1975) is made throughout this paper. The present model is different from that of Bearman & Fackrell (1975) in the following aspects:

(i) The analytical results of Parkinson & Jandali (1970) are used directly without resorting to the vortex-lattice model in Bearman & Fackrell (1975).

(ii) When the location of flow separation is known, the drag and the base pressure are determined by solving an equation derived from the similarity of pressure distributions over the body and the momentum equation by Maskell (1963) with a suitable characteristic wake width. The method is *self-contained* in comparison with Bearman & Fackrell (1975) in which the base pressure is an empirical input.

(iii) The effect of confinement has been incorporated into the present model so that the drag force can be expressed as a function of blockage ratio.

It is noted that the potential-flow model by Parkinson & Jandali (1970) has been found useful in studies of bluff-body flows such as in Durbin & Hunt (1980) and Hunt & Eames (2002). The present model is meant for providing an efficacious method for predicting the drag without being bewildered by typical shortcomings of the computational fluid dynamics method such as grid and turbulence-modelling dependence, the selection criteria of numerical convergence and lengthy computational time.

2. Disk versus flat plate

Consider a circular disk (i.e. a cone with half-apex angle $\delta = 90^\circ$) of diameter D placed symmetrically within some rigid boundaries (such as walls of a wind tunnel) of cross-sectional area A_t, as shown in figure 1(*a*). In the presence of a uniform stream

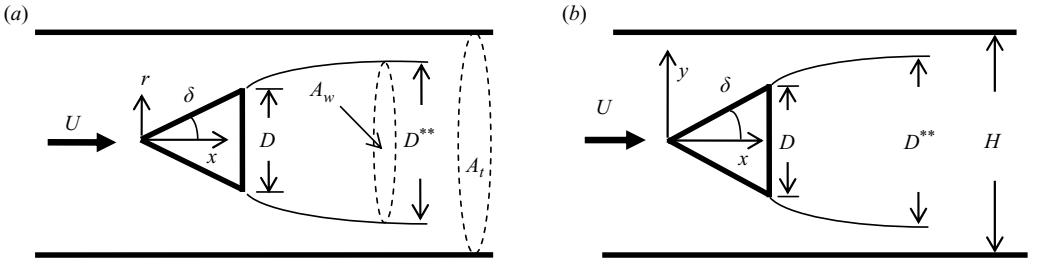

FIGURE 1. Definition sketch for (*a*) axisymmetric flow past a cone and (*b*) planar flow past a wedge.

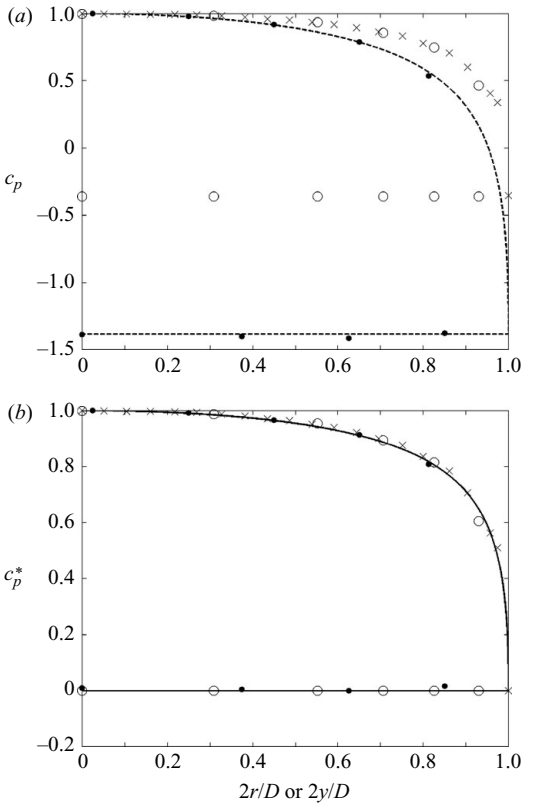

FIGURE 2. Comparison of surface pressure distributions on a disc and a flat plate normal to unconfined free stream. (*a*) c_p, (*b*) c_p^* versus $2r/D$ or $2y/D$. ○, Fail *et al.* (1957); ● , Gaster & Ponsford (1984); ×, Bearman & Fackrell (1975) ($c_{pb} = -0.36$); - - -, Parkinson & Jandali (1970) ($c_{pb} = -1.385$); ——, (2.2).

of incompressible fluid having density ρ and velocity U normal to the disk, the flow is considered potentially upstream of the disk edge and outside the shear-layer surface of characteristic wake width D^{**}, and is also axisymmetric with respect to the x-axis. The pressure variation on both faces of the disk measured by Fail, Lawford & Eyre (1957) as a function of dimensionless radial distance $2r/D$ measured from the disk centre is depicted in figure 2(*a*) in terms of the conventional pressure coefficient

c_p. The constant base pressure coefficient c_{pb} is -0.36 (corrected from -0.42 for a blockage ratio $\varepsilon = A/A_t = 1.45\,\%$, where $A = \pi D^2/4$).

Figure 1(b) defines the chord length D and the characteristic wake width D^{**} of a two-dimensional flat plate (i.e. a wedge with half-apex angle $\delta = 90^\circ$) normal to the free stream situated midway between two rigid boundaries, distant H apart. Similar to the disc, the flow on the plate is potentially upstream of separation points at its tips and outside of the shear layers, but is planar. The chordwise pressure distribution on both faces of the plate measured by Gaster & Ponsford (1984), as shown in figure 2(a) with $c_{pb} = -1.38$ (uncorrected for $\varepsilon = D/H = 1.3\,\%$), is a function of dimensionless distance $2y/D$ measured from the plate centre. The two sets of experimental data share a similar shape (i.e. c_p falling monotonically from its maximum at the frontal stagnation point and reaching its minimum *near* separation) but are different in magnitude.

The bluff-body potential-flow model for a normal flat plate in an unconfined stream by Parkinson & Jandali (1970) was recently advanced by Yeung & Parkinson (2000) such that $c_{pb} = -1.385$ is no longer an empirical input but predicted theoretically. The value is substantiated by the experimental measurements such as those by Fage & Johansen (1927), Simmons (1977) and Gaster & Ponsford (1984). The corresponding pressure distribution is shown in figure 2(a) in comparison with the numerical prediction on a circular disk by Bearman & Fackrell (1975) in which $c_{pb} = -0.36$ was specified empirically from the measurement of Fail *et al.* (1957). As in Bearman & Fackrell (1975), symbols are used to depict the computed surface pressure on the disk in figure 2(a) because they correspond to the locations of discrete vortex rings used in the vortex-lattice method. It is noted that each theoretical distribution is in good agreement with the corresponding data.

The experimental data and theoretical predictions in figure 2(a) are found to be indistinguishable after the conversion to the modified pressure coefficient

$$c_p^{\,*} = \frac{c_p - c_{pb}}{1 - c_{pb}}, \tag{2.1}$$

where individual values of c_{pb} are used, as shown in figure 2(b). Equation (2.1) may be interpreted as a renormalization under which the pressure distributions of the disk and the plate become independent of the geometry. It is important to note that $c_p^{\,*}$ is similar to the one originally proposed by Roshko & Lau (1965) to collapse the pressure distributions of *separated reattaching* flow behind a wide range of two-dimensional fore-bodies onto a single curve. To examine the wake similarity, Calvert (1967a) proposed a modified pressure coefficient to collapse the static pressure distributions in the separated-flow region behind cones of various apex angles onto a similar curve. Nonetheless, the functional forms of these curves were neither discussed nor explored in their studies. Here, (2.1) is applied to the *attached* as well as separated flows. Furthermore, the theoretical curve upstream of separation is

$$c_p^{\,*} = 1 - \frac{m^2\,(2r/D)^2}{(m + \sqrt{1 - (2r/D)^2})^2}, \quad \text{where } 0 < r < D/2, \tag{2.2}$$

which is deduced from Parkinson & Jandali (1970) (see Appendix) with $m = 1/\sqrt{1 - (-1.385)}$, and $c_p^{\,*} = 0$ downstream of separation for the two different configurations considered.

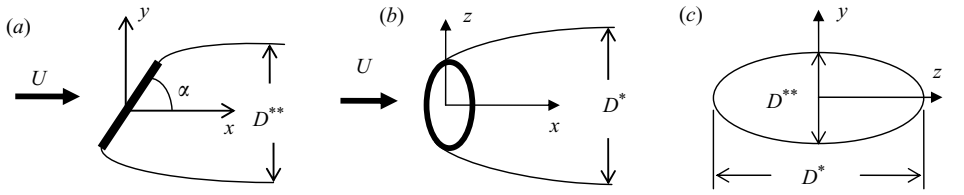

FIGURE 3. Definition sketch for flow past an inclined disk. (*a*) Plane view showing inclination α and wake width D^{**} on x–y plane, (*b*) side view showing wake width D^{*} on x–z plane, (*c*) idealized elliptical cross-section of characteristic wake on y–z plane for $\alpha < 90^{o}$.

The coefficient of form drag for the disk normal to free stream is defined as

$$c_d = \frac{2F_d}{\rho U^2 A} = 2\int_{r=0}^{D/2} (c_p - c_{pb}) \left(\frac{2r}{D}\right) \mathrm{d}\left(\frac{2r}{D}\right), \tag{2.3}$$

where F_d is the drag force. With the value of c_{pb} being unknown *a priori* and upon substituting (2.1 and 2.2) into (2.3) and carrying out the integration (see Appendix), the drag coefficient as a function of the base pressure coefficient is

$$c_d = 0.831(1 - c_{pb}). \tag{2.4}$$

It is comparable to the 'semi-empirical' relation $c_d = 0.827\ (1 - c_{pb})$ obtained by Garabedian (1956) for a disk with a cavity wake by using a different formulation. The corresponding expression for the normal plate, as derived by Yeung (2008), is

$$c_d = 0.897(1 - c_{pb}), \tag{2.5}$$

which agrees with $c_d = 0.88(1 + 0.11c_{pb}) - c_{pb}$ for a cavity model of a bluff plate obtained by Roshko (1993). To predict c_d, another relation linking the drag and base pressure is sought from the wake dynamics.

From the well-documented measurements on a disk by Calvert (1967*b*), the variation of Strouhal number $S = fD/U$ (where f is the vortex shedding frequency) with inclination α on the x–y plane defined in figure 3(*a*) is shown in figure 4(*a*). When U is replaced by the separation velocity $U_s = U\sqrt{1 - c_{pb}}$ and D is replaced by the characteristic wake width on the x–y plane,

$$D^{**} = \sqrt{2}D\sqrt{1 - c_{pb}}(\sin\alpha)^{5/2}, \tag{2.6}$$

the modified Strouhal number $S^{**} = fD^{**}/U_s \approx 0.198$ is independent of α. It is worth noting that

(*a*) $S^{**} \approx S^{*} = 0.21$, where $S^{*} = fd'/U_s$ is the wake Strouhal number by Calvert (1967*b*) with d' being 'the distance between the two major peaks of the turbulence profile',

(*b*) S^{**} is independent of c_{pb} as $S^{**} = \sqrt{2}\ S\ (\sin\alpha)^{5/2}$, and

(*c*) $D^{**} \approx d'$ in figure 4(*b*), where D^{**} is based on the experimental data of c_{pb} and (2.6).

According to the conservation of momentum by Maskell (1963), the drag coefficient is

$$c_d = (1 - c_{pb})\frac{A_w}{A} - \frac{A_w}{A}\left(1 - \frac{A_w}{A}\frac{A}{A_t}\right)^{-1}, \tag{2.7a}$$

for a bluff body of reference area A with a downstream effective wake of cross-sectional area $A_w = \pi(D^{**})^2/4$ placed within rigid boundaries, as previously defined

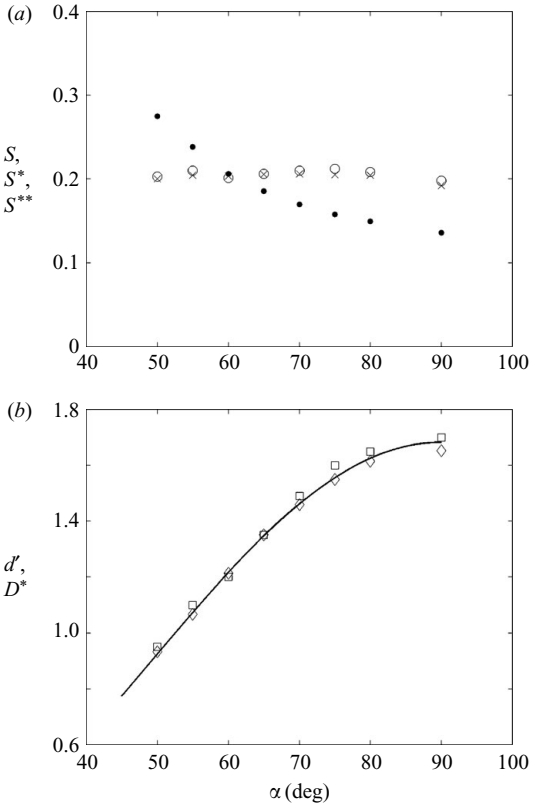

FIGURE 4. Effect of inclination α on (a) Strouhal numbers and (b) wake widths for a disc from Calvert (1967b). ●, S; ○, S^*; ×, S^{**}; □, d'; ◇, D^{**} based on measured c_{pb} and (2.6); ——, (2.6 and 2.13).

in figure 1(a). In the limit (of unconfined flow) that $A/A_t \to 0$, (2.7a) is reduced to

$$c_d = -c_{pb}\frac{A_w}{A}. \tag{2.7b}$$

It should be noted that Eppler (1954) derived the two-dimensional version of (2.7b). For a circular disk set at $\alpha = 90^\circ$ and $A_w = \pi(D^{**})^2/4$,

$$c_d = -c_{pb}(\sqrt{2}\sqrt{1-c_{pb}})^2. \tag{2.8}$$

Solving (2.4) and (2.8) simultaneously gives two possible solutions: (i) $(c_{pb}, c_d) = (1, 0)$ and (ii) $(c_{pb}, c_d) = (-0.416, 1.18)$. While the values in ($i$) are unrealistic in bluff-body flow, those in (ii) are adequate when compared with measurements of $(c_{pb}, c_d) = (-0.42, 1.12)$ (uncorrected for blockage) from Fail *et al.* (1957) and $(c_{pb}, c_d) = (-0.42, 1.18)$ from Carmody (1964). Other experimental data listed in table 1 provide further evidence to substantiate the present prediction.

The effect of wall constraint on the pressure distribution of a disk is documented in figure 5(a) by McKeon & Melbourne (1971) where a series of disks held normal to a uniform stream were tested at various values of blockage ratio $\varepsilon = A/A_t$, ranging from 1 % to 20 %. Interestingly, (2.1) is also able to collapse the experimental data onto the theoretical curve represented by (2.2), as shown in figure 5(b), where individual values

Reference	Blockage ratio (%)	c_{pb}	c_d
Hoerner (1965)	–	−0.42	1.17
Calvert (1967*a*, 1967*b*)	0.6	−0.413, −0.364	–
Roos & Willmarth (1971)	1.2	–	1.15–1.28
McKeon & Melbourne (1971)	1	−0.46	1.19
Pucher (1978)	1	−0.51	1.21
Morel *et al.* (1980)	–	−0.36	1.12
Roberts (1980)	–	−0.45	1.2
Macha *et al.* (1991)	–	–	1.158–1.168

TABLE 1. Experimental data for the disk normal to upstream flow.

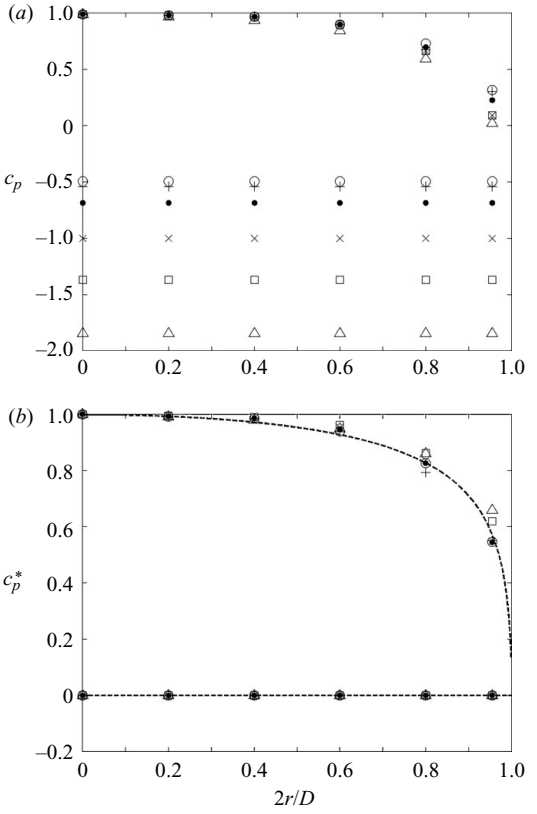

FIGURE 5. Effect of blockage on the pressure distribution of a disk normal to free stream from McKeon & Melbourne (1971). (*a*) c_p, (*b*) c_p * .○, $\varepsilon = 1\,\%$; +, 2 %; ●, 5 %; ×, 10 %; □, 15 %; △, 20 %; - - -, (2.2).

of base pressure coefficient are utilized. In other words, the renormalized pressure distributions are invariant under the blockage effect, and most importantly, (2.4) is applicable.

From Miau & Liu (1990), the measurements of Strouhal number $S = fD/U$ of a disk with Reynolds number ($Re = \rho U D/\mu$) over $10^3 \leqslant Re \leqslant 5 \times 10^4$ and $4.1\,\% \leqslant \varepsilon \leqslant 29.2\,\%$ are given in figure 6(*a*). Their data are found to be independent of ε when expressed as modified Strouhal $S^{**} = fD^{**}/U_s = 0.176$ in figure 6(*b*), if the

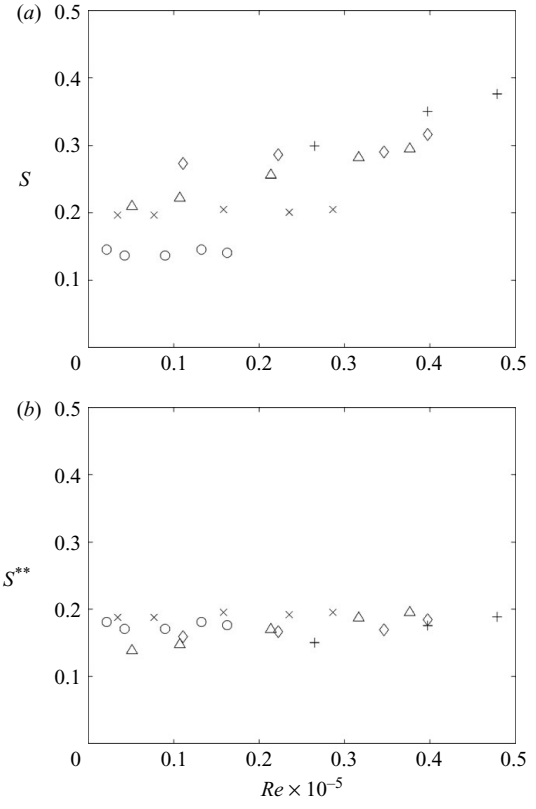

FIGURE 6. Variations of Strouhal numbers with Reynolds number (Re) and blockage ratio (ε) from Miau & Liu (1990). (a) S, (b) S^{**}.○, $\varepsilon = 4.1\,\%$; ×, 12.3 %; △, 22.3 %; ◇, 25.6 %; +, 29.2 %.

characteristic wake width is

$$D^{**} = \sqrt{2} D \sqrt{1 - c_{pb}}\,(1-\varepsilon)^3\,. \tag{2.9}$$

Substituting $A_w/A = 2(1-c_{pb})(1-\varepsilon)^6$ into (2.7a) and combining it with (2.4),

$$c_d = 0.831 \left(\frac{(1+0.831\varepsilon) - \sqrt{(1-0.831\varepsilon)^2 - 8\varepsilon(1-\varepsilon)^6}}{4\varepsilon(1-\varepsilon)^6} \right), \tag{2.10}$$

where the negative root is chosen such that in the limit $\varepsilon \to 0$, $c_d = 1.18$ as found previously. The predicted c_d and c_{pb} over $0 < \varepsilon < 25\,\%$ are plotted in figure 7, depicting the same trend as the data from McKeon & Melbourne (1971), Pucher (1978), Holst (1984), Macha *et al.* (1991) and Sumner & Brundrett (1995).

If the disk is inclined at $\alpha < 90^\circ$ in an unconfined flow, (2.4) and the condition of axisymmetry are no longer valid. The experimental measurements quoted in Hoerner (1965), however, indicate that over $45^\circ \leqslant \alpha \leqslant 90^\circ$, the normal force coefficient of the disk remains approximately constant. With the numerical constant found by the present method at $\alpha = 90^\circ$, it is appropriate to claim

$$c_d = 1.18 \sin\alpha, \tag{2.11}$$

without resorting to investigation of the pressure distribution on an inclined disk.

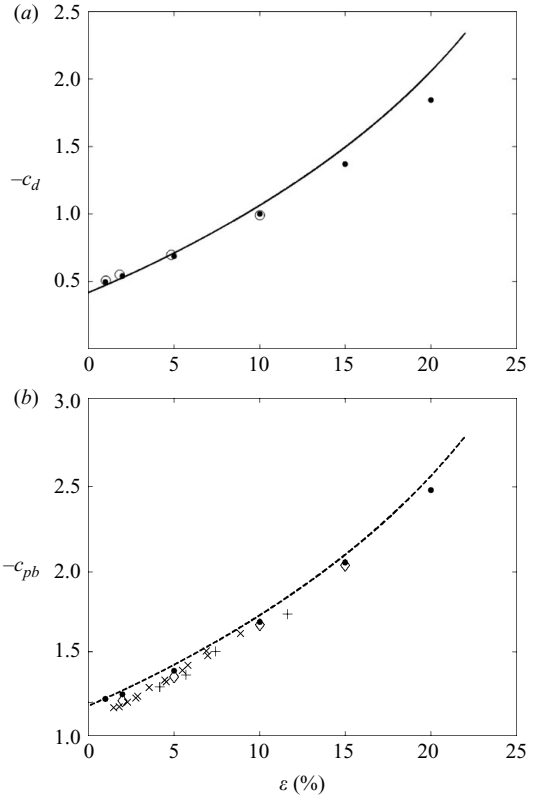

FIGURE 7. Variations of (*a*) drag and (*b*) base pressure coefficients with blockage ratio for a normal disk. ●, McKeon & Melbourne (1971); ○, Pucher (1978); +, Holst (1984); ◇, Macha *et al.* (1991); ×, Sumner & Brundrett (1995); ——, (2.10); – – –, (2.4 and 2.10).

The aforementioned wake width d' in figure 4(*b*) was obtained by Calvert (1967*b*) from the traverse of a hot wire in the y direction (defined in figure 3*a*) with x values chosen such that the static pressure reaches minimum. In the absence of axisymmetry, the wake width measured in any other plane is expected to differ from d' and 'thus the value of S^* will be different', according to Calvert (1967*b*). To idealize the wake shape for the present model, the cross-section of the characteristic wake on the y–z plane is conjectured to be an ellipse (see figure 3*c*), having D^{**} from (2.6) as the length of its minor axis in the x–y plane and D^* as that of its major axis in the x–z plane defined in figure 3(*b*). The shape of the inclined disk projected on the y–z plane is also an ellipse having $D\sin\alpha$ and D as the lengths of minor and major axes, respectively. If the two ellipses on the y–z plane are 'similar' in shape, or $D^{**}/D^* = D\sin\alpha/D$, then

$$D^* = \sqrt{2}D\sqrt{1-c_{pb}}(\sin\alpha)^{3/2}. \tag{2.12}$$

Substituting $A_w = \pi D^{**}D^*/4$ and $A = \pi D^2\sin\alpha/4$ into (2.7*b*) and solving it with (2.11),

$$c_{pb} = \frac{1-\sqrt{1+2(1.18)/\sin^2\alpha}}{2}, \tag{2.13}$$

where the positive root is ignored because it corresponds to a negative drag, being physically inadmissible. The prediction of the base pressure from (2.13) is shown in figure 8 in appropriate agreement with experimental data from Calvert (1967*a*, 1967*b*)

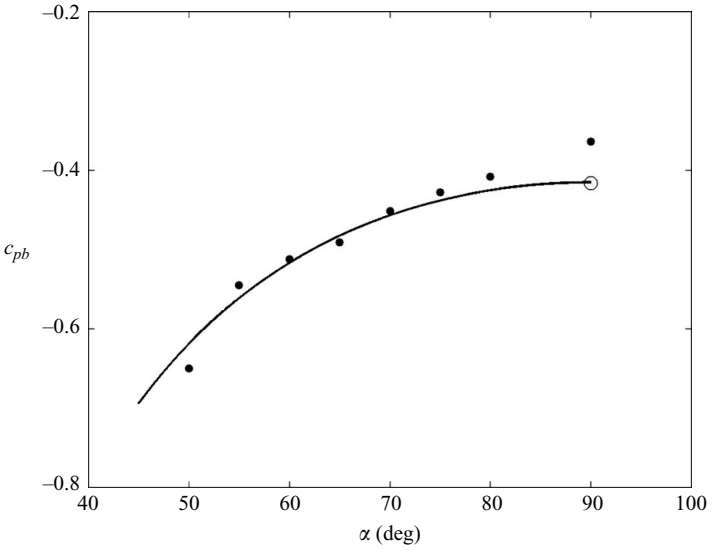

FIGURE 8. Correlation of base pressure coefficient with inclination for a disk. ●, Calvert (1967*b*); ○, Calvert (1967*a*); ——, (2.13).

where $50^\circ \leqslant \alpha \leqslant 90^\circ$. Note that two different values of c_{pb} for a disk at $\alpha = 90^\circ$ are found in Calvert (1967*a*, 1967*b*), respectively, as indicated in table 1 as well as in figure 8. In addition, D^{**} based on c_{pb} from (2.13) agrees with d' from Calvert (1967*b*), as shown in figure 4(*b*). The results in figures 4(*b*) and 8 also reflect that the conjecture of the wake shape and the method of selecting D^* are suitable.

3. Cone versus wedge

The axisymmetric flow past a cone of base diameter D and planar flow past a wedge of base thickness D, each having a half-apex angle δ, as defined in figure 1, are considered next. As demonstrated in Yeung & Parkinson (2000), the measured vortex-shedding frequency f from Simmons (1977) for wedges in unconfined flow with $10^\circ \leqslant \delta \leqslant 90^\circ$ becomes independent of δ when non-dimensionalized using

$$D^{**} = D\sqrt{1 - c_{pb}}(1 - 0.16 - 0.16\sin(2\delta + \pi/2)) \tag{3.1}$$

and velocity at separation, $U_s = U\sqrt{1 - c_{pb}}$ to form the modified Strouhal numbers $S^{**} = fD^{**}/U_s \approx 0.161$. For cones over $10^\circ \leqslant \delta \leqslant 90^\circ$, the measured variations of $S = fD/U$ and $S^* = fd'/U_s \approx 0.19$ (where d' is the measured characteristic wake width) from Calvert (1976*a*) are compared with $S^{**} = fD^{**}/U_s \approx 0.184$ in figure 9(*a*), where

$$D^{**} = \sqrt{2}D\sqrt{1 - c_{pb}}(1 - 0.19 - 0.19\sin(2\delta + \pi/2)). \tag{3.2}$$

Figure 9(*b*) clearly indicates that $D^{**} \approx d'$. Substituting $A_w/A = (D^{**}/D)^2$ into (2.7*b*),

$$c_d = -2c_{pb}(1 - c_{pb})(1 - 0.19 - 0.19\sin(2\delta + \pi/2))^2. \tag{3.3}$$

Since the experimental measurements of pressure distribution for incompressible flow past a cone are rarely reported in the literature, it is not possible to demonstrate the invariance of pressure distributions between the wedges and the cones here.

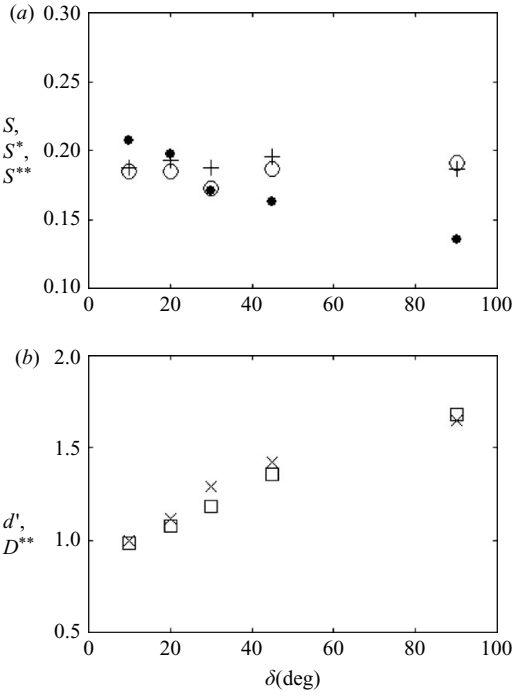

FIGURE 9. Variations of (*a*) Strouhal numbers and (*b*) wake widths for a cone of half-apex angle δ from Calvert (1967*a*). ●, S; +, S^*; ○, S^{**}; ×, d'; □, D^{**}.

However, if such invariance exists, a linear equation linking the base pressure and form drag coefficients can be established as

$$c_d = (1 - c_{pb})F(\delta), \tag{3.4}$$

where $F(\delta)$ is a function of δ for cones (see figure 10*a*) by using the potential-flow model for wedges of arbitrary δ developed by Yeung & Parkinson (2000). Solutions of $(-c_{pb}, c_d)$ obtained by solving (3.3) and (3.4) are compared with data from Calvert (1976*a*) and Hoerner (1965) for a range of δ in figure 10(*b*). Following (2.9), a characteristic wake width including the blockage effect is

$$D^{**} = \sqrt{2}D\sqrt{1 - c_{pb}}(1 - 0.19 - 0.19\sin(2\delta + \pi/2))(1 - \varepsilon)^3. \tag{3.5}$$

By combining (2.7*a*), (3.4) and (3.5), variations of the drag coefficient as functions of the blockage ratio for $\delta = 10^\circ$, 30° and 60° are shown in figure 10(*c*), indicating that the effect of blockage is almost negligible when $\delta \leqslant 10^\circ$.

4. Sphere versus cylinder

4.1. *Subcritical flow region*

Consider a sphere and a circular cylinder, each of diameter D, approached by a uniform flow, as shown in figure 11, where angle β is measured from the frontal stagnation point. It is well known that the angular location of flow separation β_s and the base pressure c_{pb} are strongly influenced by the Reynolds number. Figure 12(*a*) compares the measured pressure distributions in terms of c_p on a sphere by Fage (1937) at $Re = 1.57 \times 10^5$ and on a circular cylinder by Roshko (1954)

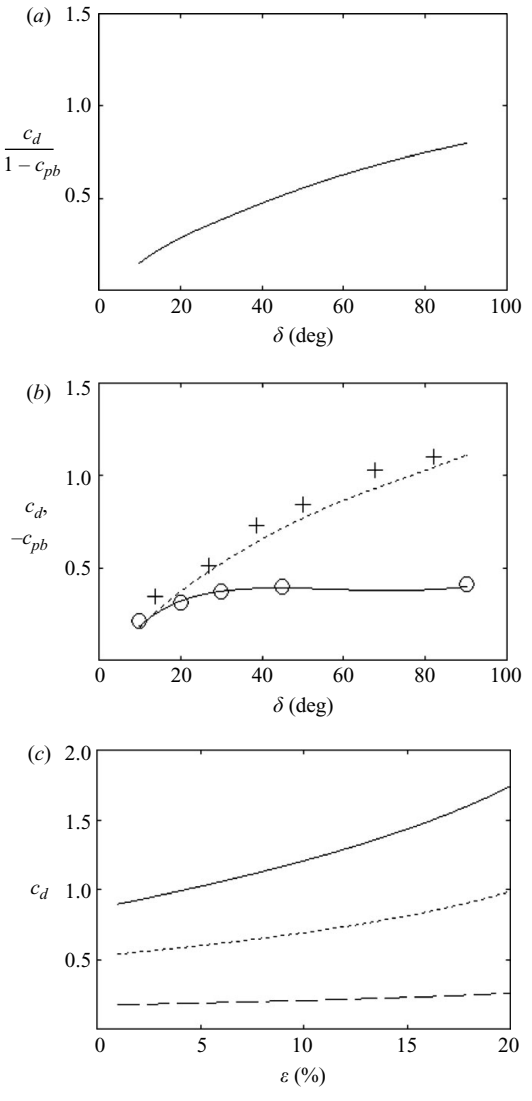

FIGURE 10. Variations of drag and base pressure coefficients for a cone of half-apex angle δ. (*a*) $c_d/(1-c_{pb})$, (*b*) $-c_{pb}$: ○, Calvert (1967*a*); ——, present; c_d: +, Hoerner (1965); - - -, present; (*c*) c_d——, $\delta = 60$ deg, - - -, 30 deg, – – –, 10 deg.

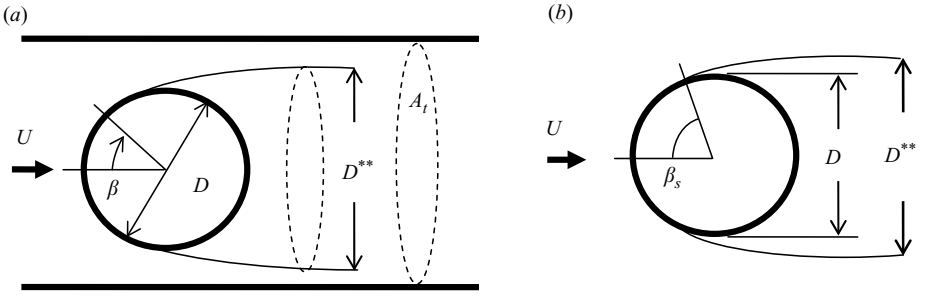

FIGURE 11. Definition sketch for (*a*) axisymmetric flow past a sphere and (*b*) planar flow past a circular cylinder, each of diameter D.

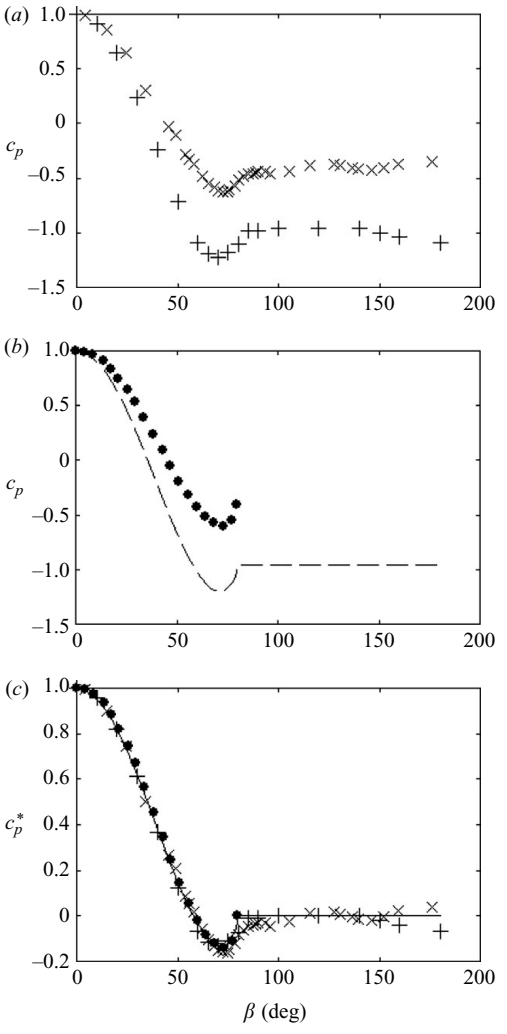

FIGURE 12. Comparison of surface pressure distributions of a sphere and a circular cylinder with laminar separation. (*a, b*) c_p versus β; (*c*) c_p^* versus β. ×, Fage (1937); +, Roshko (1954); ●, Bearman & Fackrell (1975); – – –, Parkinson & Jandali (1970) ($c_{pb} = -0.938$, $\beta_s = 80$deg); ——, (4.1).

at $Re = 1.45 \times 10^4$, representing the typical subcritical Reynolds numbers in which laminar boundary layer separation takes place nearly at $\beta_s = 80°$. The base pressure of the sphere ($c_{pb} = -0.4$) is less negative than that of the cylinder ($c_{pb} = -0.94$). The theoretical pressure distribution on a circular cylinder with $\beta_s = 80°$ and $c_{pb} = -0.938$ (see the Discussion section for the detailed calculation) is compared with the numerical prediction on a sphere from Bearman & Fackrell (1975) with $\beta_s = 80°$ and $c_{pb} = -0.4$ (provided by experiment) in figure 12(*b*). Again, symbols are used to depict the computed surface pressure by Bearman & Fackrell (1975) on the sphere in figure 12(*b*) because they correspond to the locations of discrete vortex rings used in their numerical method.

Under the transformation in (2.1), the distributions in figure 12(a, b) are collapsed onto

$$c_p^* = \begin{cases} 1 - \dfrac{\sin^2\theta(1 - 2\cos\alpha_s\cos\theta + \cos^2\alpha_s)^2}{m^2(\cos\delta - \cos\theta)^2} & \alpha_s \leqslant \theta < 180^\circ, \\ 0 & 0 \leqslant \theta \leqslant \alpha_s, \end{cases} \tag{4.1}$$

which was modified from Parkinson & Jandali (1970) for a circular cylinder with $\beta_s = 80^\circ$, $m = 1/\sqrt{1-(-0.938)}$, $\alpha_s = (180^\circ - \beta_s)/2$, $\sin\beta = \cos\alpha_s \sin\theta(\sec\alpha_s - \cos\theta)/[(\sec\alpha_s + \cos\alpha_s)/2 - \cos\theta]$ and $\cos\delta = \cos\alpha_s + m\sin^3\alpha_s$, as shown in figure 12($c$). Making use of (2.1), the coefficient of form drag for the sphere becomes

$$c_d = 2\int_{\beta=0}^{\pi} c_p \cos\beta \sin\beta \,\mathrm{d}\beta = (1 - c_{pb}) \int_{\beta=0}^{\beta_s} c_p^* \sin 2\beta \,\mathrm{d}\beta, \tag{4.2}$$

where c_{pb} is considered as an unknown. By carrying out the integration and by using (4.1), it is found that

$$c_d = 0.317(1 - c_{pb}). \tag{4.3}$$

Möller (1938) is usually quoted as the earliest to realize that two Strouhal numbers exist in the wake of a sphere when the Reynolds number falls in the range of $10^3 < Re < 10^4$. It is the lower value $S = 0.188$ that is reported by Calvert (1972) together with $c_{pb} = -0.35$ in $2 \times 10^4 < Re < 6 \times 10^4$. Based on the maximum wake width measured ($d' = 1.12D$) and the velocity outside the wake ($U_s \approx 1.09U$), a wake Strouhal number S^* of 0.193 was thus obtained. As elaborated in the Discussion, $D^{**} = (S^*/S)\sqrt{1 - c_{pb}} D \sin\beta_s$ is proposed for the circular cylinder. Realizing $S^*/S \approx 1$, a characteristic wake width for the sphere is proposed as

$$D^{**} = \sqrt{1 - c_{pb}} D \sin\beta_s, \tag{4.4}$$

where $D\sin\beta_s$ is interpreted as the projected diameter of the sphere. By substituting $A_w = \pi(D^{**})^2/4$ into (2.7b),

$$c_d = -c_{pb}(1 - c_{pb}) \sin^2\beta_s. \tag{4.5}$$

The experimental data from Flachsbart (1927), Fage (1937), Maxworthy (1969) and Achenbach (1972) in figure 13(a) are reasonably close to the solution $(c_{pb},\ c_d) = (-0.33,\ 0.42)$ from solving (4.3) and (4.5) with the discrepancy attributed to the fact that (2.7a) does not include frictional drag.

Maxworthy (1969) studied the effect of confinement on the pressure distribution of a sphere with laminar separation. Figure 14(a) compares the c_p distributions at area blockage ratio $\varepsilon = 5\,\%$ and 25 % where $Re \approx 2 \times 10^5$. After the conversion to c_p^*, both distributions are reasonably represented by the curve from (4.1), as shown in figure 14(b), indicating the existence of similarity in pressure distributions under the influence from blockage effect.

To the author's knowledge, experimental data of Strouhal number for a sphere in the presence of confinement are scarce in the literature. To identify the characteristic wake width, experimental data for a flat plate, a circular cylinder and a disk are considered. The data of S in figure 15(a) from Shaw (1971) for a normal flat plate become approximately independent of blockage ratio ε when expressed as

$$S^{**} = S(1 - \varepsilon)^{3/2}. \tag{4.6}$$

Additional comparisons with data from other sources to deduce (4.6) are available in Yeung (2008). The corresponding expression for the data in figure 15(b) from Richter

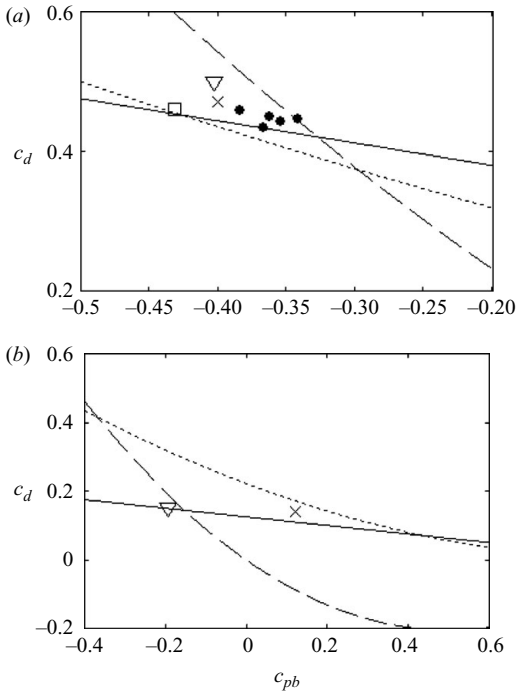

FIGURE 13. Predictions of base pressure and drag coefficients for a sphere. (*a*) subcritical ($\beta_s = 80$deg), ——, (4.3); (*b*) supercritical ($\beta_s = 115$deg), ——, (4.11). □, Flachbart (1927); × : Fage (1937); ●, Maxworthy (1969); ▽, Achenbach (1972); – – –, (4.5); - - -, (5.3).

and Naudascher (1976) for a circular cylinder at $10^4 < Re < 10^5$ is

$$S^{**} = \frac{0.16 \sin 80^\circ}{0.2} S(1-\varepsilon), \tag{4.7}$$

where 0.2 is assumed to be the Strouhal number when $\varepsilon = 0$, 0.16 is the universal Strouhal number by Roshko (1954) and $\beta_s = 80^\circ$. From figure 6, it is found that for a disk,

$$S^{**} = \sqrt{2} S(1-\varepsilon)^3. \tag{4.8}$$

While a flat plate and a disk have flat surfaces, those of a circular cylinder and a sphere are curved. Based on the similar functional dependence of $(1-\varepsilon)$ in (4.6)–(4.8), it is conjectured that the confinement effect on flat surfaces is 'similar' to that on curved surfaces. That is, the change of exponents in $(1-\varepsilon)$ from the flow past a plate to the flow past a disk is 'equal' to the corresponding change from the flow past a cylinder to the flow past a sphere: $3 - 3/2 = n - 1$ or $n = 5/2$ where n is the exponent of $(1-\varepsilon)$ for the sphere. Incorporating it into (4.4),

$$D^{**} = \sqrt{1 - c_{pb}} D \sin \beta_s (1-\varepsilon)^{5/2}. \tag{4.9}$$

Substituting $A_w/A = (D^{**}/D)^2$ into (2.7*a*) and solving it with (4.3),

$$c_d = 0.317 \left(\frac{(1 + 0.317\varepsilon) - \sqrt{(1+0.317\varepsilon)^2 - 4\varepsilon(0.317 + \sin^2 \beta_s (1-\varepsilon)^5)}}{2\varepsilon \sin^2 \beta_s (1-\varepsilon)^5} \right). \tag{4.10}$$

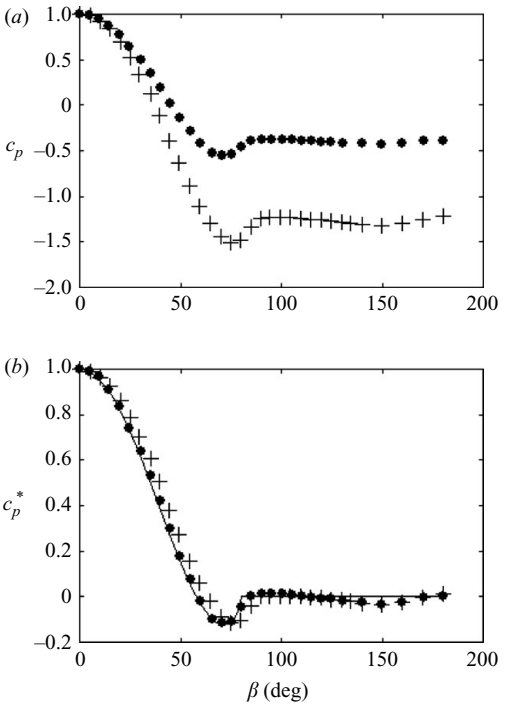

FIGURE 14. Effect of blockage on the pressure distribution of a sphere at $Re \approx 2 \times 10^5$ from Maxworthy (1969). (*a*) c_p versus β; (*b*) c_p^* versus β. •, $\varepsilon = 5\,\%$; +, 25 %; ——, (4.1).

A comparison is made in figure 16 between experimental data from Maxworthy (1969), Achenbach (1974) and Awbi & Tan (1981) and the prediction from (4.10), substantiating the choice of the exponent deduced from similarity as proposed.

4.2. *Supercritical flow region*

For the case with turbulent boundary layer separation, the data from Achenbach (1972) on a sphere at $Re = 1.14 \times 10^6$ and that from Achenbach (1968) on a circular cylinder at $Re = 3.6 \times 10^6$ are compared in figure 17(*a*). While the angle of separation is approximately $\beta_s = 115^\circ$ in each case, it is found that $(c_{pb}, c_d) = (-0.2, 0.15)$ for the sphere but $(c_{pb}, c_d) = (-0.85,\ 0.75)$ for the cylinder. It is noted that for the cylinder, the base pressure may be accurately calculated from $c_{pb} = 1 - (9/4)\sin^2\beta_s$, which corresponds to satisfying the criterion of finite streamline curvature at separation found in Parkinson & Jandali (1970). As shown, the theoretical pressure distribution from Parkinson & Jandali (1970) agrees with the experimental data for the circular cylinder but differs from that of the sphere. To avoid the effect of a separation bubble on the pressure distribution, the data from Fage (1937) for a sphere at $Re = 1.1 \times 10^5$ (and the corresponding numerical prediction from Bearman & Fackrell (1975)) are not used for comparison. When expressed in terms of c_p^*, the experimental distributions are in satisfactory agreement with the theoretical curve (obtained from (4.1) with $m = 1/\sqrt{1-(-0.85)}$ and $\beta_s = 115^\circ$) in figure 17(*b*). From (4.2),

$$c_d = 0.125(1 - c_{pb}). \tag{4.11}$$

If the characteristic wake width in (4.4) is still valid with $\beta_s = 115^\circ$, then the solution of (4.5) and (4.11) is $(c_{pb},\ c_d) = (-0.15,\ 0.144)$ in reasonable agreement with the data

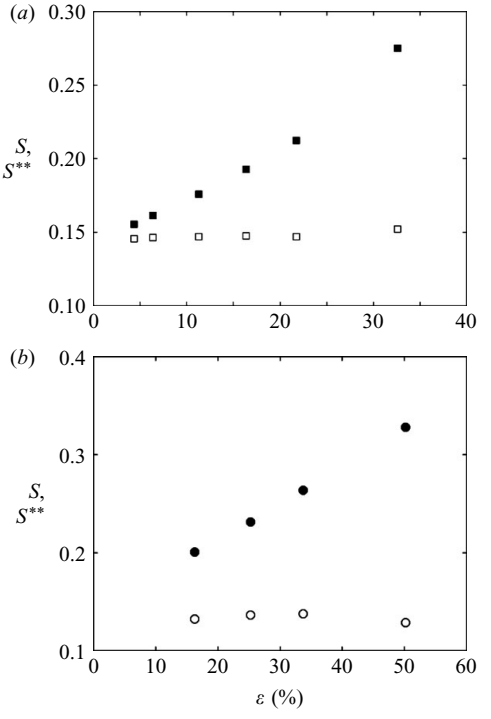

FIGURE 15. Variations of Strouhal numbers with blockage ratio for (*a*) a normal flat plate from Shaw (1971) and (*b*) a circular cylinder from Richter and Naudascher (1976) at subcritical flow. ■, ●, S; □, ○, S^{**}.

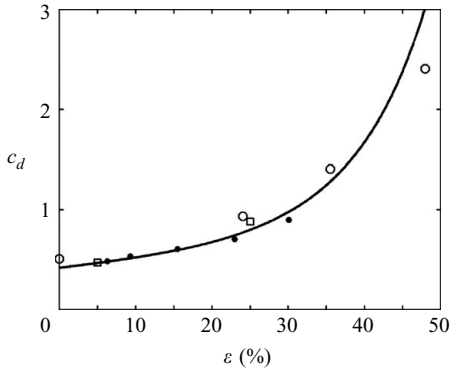

FIGURE 16. Variation of drag coefficient on a sphere with blockage ratio. □, Maxworthy (1969); ○, Achenbach (1974); ●, Awbi & Tan (1981); ——, (4.10).

from Achenbach (1972), as shown in figure 13(*b*). The equation of drag as a function of blockage ratio can be easily obtained by replacing 0.317 in (4.10) by 0.125, which is the numerical constant in (4.11).

5. Discussion

The linear relation between the base pressure and the drag coefficients in (2.4) is derived under the assumption that the pressure distribution on the disk is

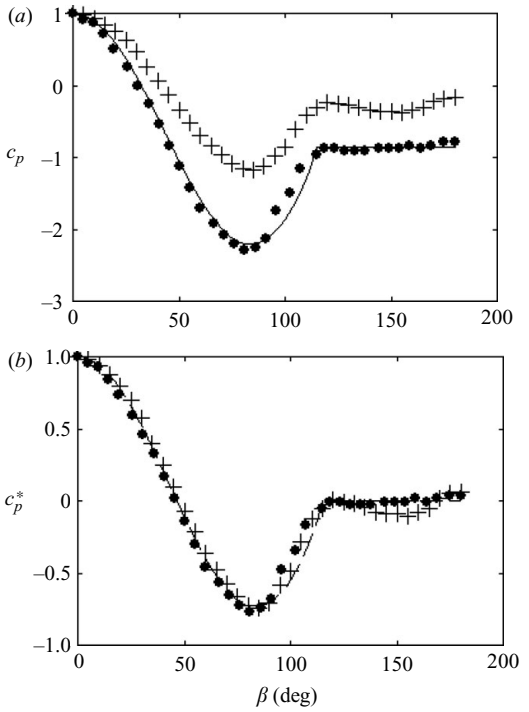

FIGURE 17. Comparison of surface pressure distributions of a sphere and a circular cylinder with turbulent separation. (*a*) c_p versus β, (*b*) c_p^* versus β. ●, Achenbach (1968); +, Achenbach (1972); ——, Parkinson & Jandali (1970) ($c_{pb} = 1 - (9/4)\sin^2\beta_s$, $\beta_s = 115$deg); – – –, (3.5).

axisymmetric. Interestingly, it is not much different from $c_d = 0.837\ (1 - c_{pb})$ for *square* plates (where the pressure distribution is not axisymmetric) deduced by Maskell (1963) from the experimental data over a wide range of conditions. Therefore, it agrees with Fail *et al.* (1957) that 'large changes in the shape of low-aspect-ratio plates have very small effects on the aerodynamic characteristics'. In addition, (2.4) and (2.5)

(*a*) provide the correct limits theoretically to the experimental data from Fail *et al.* (1957) for rectangular plates at aspect ratio $1 \leqslant AR < \infty$ in figure 18(*a*),

(*b*) describe the correct trend of experimental data on square plates from Bearman (1971) and a square prism normal to free stream from Lee (1975) in turbulent flow in figure 18(*b*) and

(*c*) are applicable to the data from Apelt & West (1975) for a flat plate with a wake splitter plate in figure 18(*c*).

As such, the present method may be suitable for estimating the drag on these bluff bodies.

In Yeung (2008), the momentum equation by Maskell (1963) was modified to study the two-dimensional flow around an inclined flat plate in confined flow. After combining it with another equation derived from the potential flow model by Parkinson & Jandali (1970), c_{pb} may be determined by a nonlinear equation numerically. For the inclined disk in unconfined flow considered here, the equation from Parkinson & Jandali (1970) cannot be used. Instead, the experimental measurements which are documented in Hoerner (1965) prove to be useful. It is shown here that c_{pb} may be determined by solving a quadratic equation.

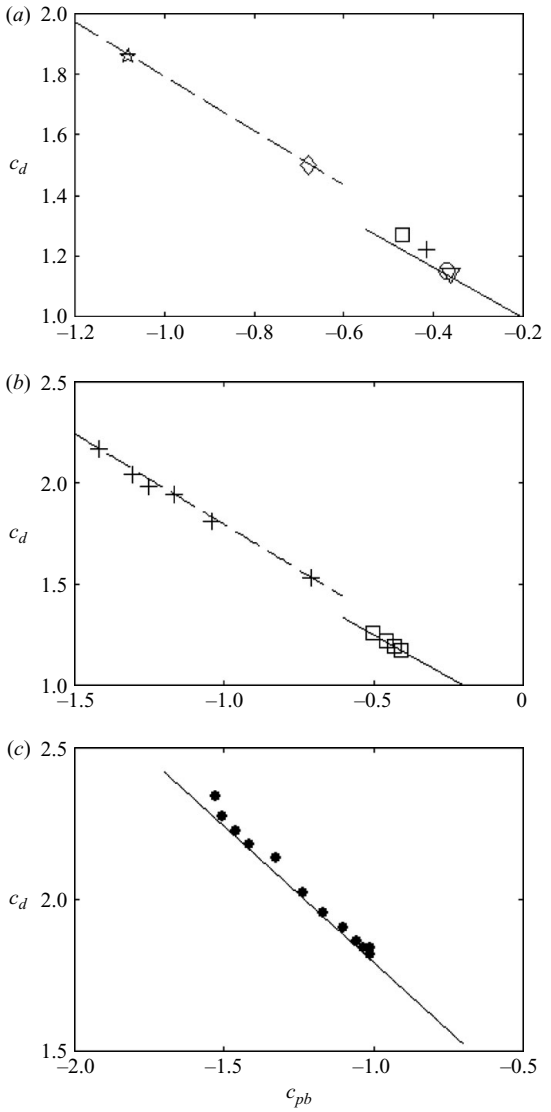

FIGURE 18. Correlation between base pressure and drag for flat plates. (*a*) Smooth flow: ☆, two-dimensional; ◇, $AR = 20$; □, $AR = 10$; +, $AR = 5$; ○, $AR = 2$; ▽, $AR = 1$ from Fail *et al.* (1957), (*b*) turbulent flow: □, square plate from Bearman (1971); +, square prism from Lee (1975); (*c*) flat plate with splitter plate from Apelt & West (1975); ——, (2.4); – – –, (2.5).

The confined flow past a circular cylinder at subcritical Reynolds numbers was also considered in Yeung (2008). The base pressure coefficient and the location of flow separation are assumed to be $(c_{pb},\ \beta_s) = (-0.96,\ 80^\circ)$, which are the measurements of Roshko (1954) used by Parkinson & Jandali (1970). An attempt is made here to eliminate the empirical input, namely c_{pb}. As elucidated in Parkinson & Jandali (1970), theoretical models for flows past bluff bodies include some empiricism because of the complexity of the wake dynamics. For the flow past a circular cylinder, the angle of flow separation β_s and the base pressure c_{pb} are such parameters in the model obtained from experiments. Based on the separation velocity $U\sqrt{1 - c_{pb}}$ and the wake width

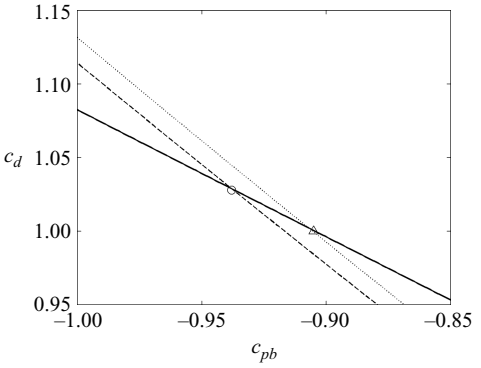

FIGURE 19. Relations between base pressure and drag coefficients for a circular cylinder at subcritical flow region. ——, (4.8) from Parkinson & Jandali (1970) ($\beta_s = 80$deg); – – –, (5.1); - - -, (5.2); ○: solution of (4.8) from Parkinson & Jandali (1970) and (5.1); Δ: solution of (4.8) from Parkinson & Jandali (1970) and (5.2).

d' from a modified Kirchhoff's free streamline model, a universal Strouhal number $S^* = Sd'/(D\sqrt{1-c_{pb}}) \approx 0.16$ for all cylinders was proposed by Roshko (1954). If the characteristic wake width is assumed to be $D^{**} = d' \sin\beta_s$, then from (2.7*b*)

$$c_d = -c_{pb}\frac{S^*}{S}\sqrt{1-c_{pb}}\sin\beta_s. \tag{5.1}$$

From Roshko (1954), $S \approx 0.2$ at $Re = 1.49 \times 10^4$, a typical subcritical Reynolds number. Another expression of drag can be obtained from integrating the pressure distribution to give $c_d = 2\int_{\beta=0}^{\pi} c_p \cos\beta \, \mathrm{d}\beta$ or use (4.8) from Parkinson & Jandali (1970). The solution of (5.1) and (4.8) from Parkinson & Jandali (1970) is depicted in figure 19 at $(c_{pb}, c_d) = (-0.938,\ 1.03)$, given $\beta_s = 80^\circ$. If $D^{**} = d'$ instead, then from (2.7*b*)

$$c_d = -c_{pb}\frac{S*}{S}\sqrt{1-c_{pb}}. \tag{5.2}$$

The solution of (5.2) and (4.8) from Parkinson & Jandali (1970) is shown in figure 19 at $(c_{pb}, c_d) = (-0.905,\ 1.0)$, which is less accurate when compared with $(c_{pb}, c_d) = (-0.94,\ 1.15)$ from the measurements by Roshko (1954). Therefore, if the proposed theoretical wake width is suitable, then only the angle of flow separation is needed in the model by Parkinson & Jandali (1970) for the subcritical flow past the circular cylinder. Incidentally, from the measurements of Roshko (1961) at $Re = 8.4 \times 10^6$ (i.e. trans-critical), $(c_{pb}, c_d) = (-0.86,\ 0.70)$. With $\beta_s \approx 104^\circ$ deduced from the measured pressure distribution, (5.1) predicts $S = 0.26$, which is reasonable when compared with the measured value of $S = 0.267$.

The experimental studies of blockage effect on the Strouhal number for two-dimensional bluff bodies have been well documented. However, a theoretical prediction of its variation in confined flow is not available in the literature. Therefore, the present method makes use of the experimental measurements for the normal disk to establish the characteristic wake width such as (2.9). Here, the continuity equation is first used to deduce the important parameter $(1-\varepsilon)$ for blocked flow. Only its exponent is to be determined next. Interestingly, this simple functional dependence, namely $(1-\varepsilon)^n$, where n depends on the geometry, leads to realistic results for the variety of bluff bodies considered. Furthermore, experimental studies of blockage effect on the Strouhal number for three-dimensional bodies are limited. It has been shown in the present study that the data for the flat-plate circular cylinder and the

disk can be used to deduce the theoretical wake width for the sphere such that the form drag on a sphere in confined flow can be determined. Based on potential flow, Hoerner (1965) developed an expression,

$$c_d = \frac{2}{9}(1 - c_{pb})^2, \tag{5.3}$$

for determining the sphere drag based on a single point measurement of base pressure (see Platt 1937 for derivation). Good correlation with experimental data is also quoted therein. The solution from solving (4.3) and (5.3) is in reasonable agreement with experimental data shown in figure 13(*a*) at subcritical Reynolds numbers but the base pressure from (4.11) and (5.3) is more positive than those from the measurements by Fage (1937) and Achenbach (1972) in figure 13(*b*) at supercritical Reynolds numbers. As the blockage ratio is not involved explicitly in (5.3), it is not obvious if (5.3) is applicable to confined flow.

6. Conclusion

A simple method is presented to calculate the drag and the base pressure on a bluff body such as a disk, a cone, a circular cylinder and a sphere in confined flow. It is based on (*i*) the invariance of pressure distribution, (*ii*) the potential-flow model by Parkinson & Jandali (1970), (*iii*) a characteristic wake width and (*iv*) the momentum equation by Maskell (1963). Analytical expressions for the drag as a function of the blockage ratio have been derived. For the disk and the cone, the model is self-contained. For the sphere, the drag and the base pressure depend on the location of flow separation. In general, the prediction is in reasonable agreement with experimental data. A characteristic wake width based on the universal Strouhal number by Roshko (1954) is proposed for the subcritical flow past a circular cylinder such that the base pressure in the potential-flow model is no longer an empirical input but determined theoretically. The Strouhal number obtained from the momentum equation and this characteristic wake width are consistent with the measurement by Roshko (1961) for trans-critical flow. The method presented here may be applied to other two-dimensional and axisymmetric bluff bodies as long as they are of comparable bluffness and they are associated with a broad wake downstream of separation such that the pressure drag dominates.

The author would like to dedicate this paper to the memory of Professor Geoffrey Parkinson (1924–2005) and thank the referees for their comments.

Appendix

According to (3.6) of Parkinson & Jandali (1970), the pressure distribution on a normal flat plate is given by

$$c_p = 1 - \frac{\sin^2\theta}{(\cos\delta - \cos\theta)^2}, \tag{A 1}$$

where $2y = D\sin\theta$ and $\cos\delta = 1/\sqrt{1 - c_{pb}}$. For unconfined flow, Yeung & Parkinson (2000) found that $c_{pb} = -1.385$. On the wetted surface, $\pi/2 < \theta < \pi$, so $\cos\theta = -\sqrt{1 - \sin^2\theta}$. Substituting (A1) into (2.1),

$$c_p^* = 1 - \frac{m^2 Z^2}{(m + \sqrt{1 - Z^2})^2}, \tag{A 2}$$

where $Z = 2y/D$ and $m = 1/\sqrt{1-(-1.385)}$. The drag coefficient is

$$c_d = \frac{2}{D}\int_{y=0}^{D/2}(c_p - c_{pb})\,\mathrm{d}y = (1-c_{pb})\int_{Z=0}^{1} c_p\,\mathrm{d}Z. \tag{A 3}$$

Integration gives

$$\int_{Z=0}^{1}\left(1-\frac{m^2Z^2}{(m+\sqrt{1-Z^2})^2}\right)\mathrm{d}Z = 2m^2 - m^3\pi + 1 + \frac{m^2(2m^2-1)}{\sqrt{1-m^2}} \times \tanh^{-1}\sqrt{1-m^2} = 0.8967.$$

The drag coefficient for the disk is

$$c_d = 2\,(1-c_{pb})\int_{r=0}^{D/2} c_p^*\left(\frac{2r}{D}\right)\mathrm{d}\left(\frac{2r}{D}\right). \tag{A 4}$$

Substituting (A2) and $Z = 2r/D$ into (A 4),

$$c_d = 2\,(1-c_{pb})\int_{Z=0}^{1} c_p{}^*\,Z\mathrm{d}Z. \tag{A 5}$$

Integration gives

$$\int_{z=0}^{1}\left[Z-\frac{m^2Z^3}{(m+\sqrt{1-Z^2})}\right]\mathrm{d}Z = \frac{1}{2} - 3m^3 + \frac{3m^2}{2} - (1-3m^2)m^2\ln\left(\frac{m+1}{m}\right) = 0.8308.$$

REFERENCES

Achenbach, E. 1968 Distribution of local pressure and skin friction around a circular cylinder in cross-flow up to $Re = 5\times10^6$. *J. Fluid Mech.* **34**, 625–639.

Achenbach, E. 1972 Experiments on the flow past spheres at very high Reynolds numbers. *J. Fluid Mech.* **54**, 565–575.

Achenbach, E. 1974 The effects of surface roughness and tunnel blockage on the flow past spheres. *J. Fluid Mech.* **65**, 113–125.

Apelt, C. J. & West, G. S. 1975 The effects of wake splitter plates on bluff-body flow in the range $10^4 < R < 5\times10^4$. Part 2. *J. Fluid Mech.* **71**, 145–160.

Awbi, H. B. & Tan, S. H. 1981 Effect of wind-tunnel walls on the drag of a sphere. *J. Fluids Engng* **103**, 461–465.

Bearman, P. W. 1967 On vortex street wakes. *J. Fluid Mech.* **28**, 625–841.

Bearman, P. W. 1971 An investigation of the forces on flat plates normal to a turbulent flow. *J. Fluid Mech.* **46**, 177–198.

Bearman, P. W. 1998 Developments in the understanding of bluff body flows. *JSME* B **41**, 103–114.

Bearman, P. W. & Fackrell, J. E. 1975 Calculation of two-dimensional and axi-symmetric bluff-body potential flow. *J. Fluid Mech.* **72**, 229–241.

Calvert, J. R. 1967*a* Experiments on the low-speed flow past cones. *J. Fluid Mech.* **27**, 273–289.

Calvert, J. R. 1967*b* Experiments on the flow past an inclined disk. *J. Fluid Mech.* **29**, 691–703.

Calvert, J. R. 1972 Some experiments on the flow past a sphere. *Aeronaut. J.* **76**, 248–250.

Carmody, T. 1964 Establishment of the wake behind a disk. *Trans. ASME: J. Fluids Engng* **86**, 869–882.

Durbin, P. A. & Hunt, J. C. R. 1980 On surface pressure fluctuations beneath flow round bluff bodies. *J. Fluid Mech.* **100**, 161–184.

Eppler, R. 1954 Contributions to the theory and applications of discontinuous flows. *J. Ration. Tech. Anal.* **3**, 591–644.

Fage, A. 1937 Experiments on a sphere at critical Reynolds numbers. *Aero. Res. Counc. Rep. and Memo.* no. 1766 (see Goldstein S. 1965 *Modern developments in fluid dynamics*, vol. 2, 497).

Fage, A. & Johansen, F. C. 1927 On the flow of air behind an inclined flat plate of infinite span. *Proc. R. Soc. Lond.* A **116**, 170–197.

Fail, R., Lawford, J. A. & Eyre, R. C. W. 1957. Low-speed experiments on the wake characteristics of flat plates normal to an air stream. *Aero. Res. Counc. R. & M.* no. 3120.

Flachsbart, O. 1927. Neue Untersuchungen über den Luftwiderstand con Kugeln. *Physikalische Zeitschrift*, **28**, 461–469 (see *NACA TM 475*).

Fornberg, B. 1988. Steady viscous flow past a sphere at high Reynolds numbers. *J. Fluid Mech.* **190**, 471–489.

Garabedian, P. R. 1956 Calculation of axially symmetric cavities and jets. *Pac. J. Math.* **6**, 611–684.

Gaster, M. & Ponsford, P. J. 1984. The flows over tapered flat plates normal to the stream. *Aeronaut. J.* **88**, 206–212.

Hoerner, S. F. 1965. *Fluid-Dynamic Drag*. Hoerner Fluid Dynamics. .

Hoffman, J. 2006 Adaptive simulation of the subcritical flow past a sphere. *J. Fluid Mech.* **568**, 77–88.

Holst, H. 1984. Wind tunnel wall interference in closed, ventilated and adaptive test sections. *NASA* CP-2319, 61–78.

Hunt, J. C. R. & Eames, I. 2002 The disappearance of laminar and turbulent wakes in complex flows. *J. Fluid Mech.* **457**, 111–132.

Lee, B. E. 1975 The effect of turbulence on the surface pressure field of a square prism. *J. Fluid Mech.* **69**, 263–282.

Macha, J. M., Buffington, R. J. & Henfling, J. F. 1991 Slotted-wall blockage corrections for disks and parachutes. *J. Aircr.* **28**, 592–597.

Maskell, E. C. 1963 A theory of the blockage effects on bluff bodies and stalled wings in a closed wind tunnel. *Aero. Res. Counc. R. & M.* no. 3400.

Masliyah, J. H. & Epstein, N. 1970 Numerical study of steady flow past spheroids. *J. Fluid Mech.* **44**, 493–512.

Maxworthy, T. 1969 Experiments on the flow around a sphere at high Reynolds numbers. *J. Appl. Mech., Trans. ASME* E **36**, 598–607.

McKeon, R. J. & Melbourne, W. H. 1971 Wind tunnel blockage effects and drag on bluff bodies in a rough wall boundary layer. In *Proceedings of the Third International Conference of Wind Effects on Buildings and Structures*, Tokyo, Japan, 263–272.

Miau, J. J. & Liu, T. W. 1990 Vortex flowmeter designed with wall pressure measurement. *Rev. Sci. Instrum.* **61** (10), 2676–2681.

Möller, W. 1938 Experimentelle Untersuchung zur Hydromechanik der Kugel. *Phys. Z.* **39**, 57–80.

Morel, T. & Bohn, M. 1980 Flow over two circular disks in tandem. *Trans. ASME I: J. Fluids Engng* **102**, 104–111.

Parkinson, G. V. & Jandali, T. 1970 A wake source model for bluff body potential flow. *J. Fluid Mech.* **40**, 577–594.

Pitter, R. L., Pruppacher, H. R. & Hamielec, A. E. 1973 A numerical study of viscous flow past thin oblate spheroid at low and intermediate Reynolds numbers. *J. Atmos. Sci.,* **30,** 125–134.

Platt, R. C. 1937 Turbulence factors of N.A.C.A. wind tunnels as determined by sphere tests. *NACA Report* 558.

Pucher, P. 1978 Experimetelle Untersuchung an Würfeln und Quadern zur Bestimmung des Versperrungseinflusses in Windkanälen mit offener Meßstrecke. PhD thesis, TU MÜnchen, (see Kramer, C., Gerhardt, H. J. & Regenscheit, B. *J. Wind Engng Ind. Aerodyn.* **16** (1984), 225–264).

Richter, A. & Naudascher, E. 1976 Fluctuating forces on a rigid cylinder in confined flow. *J. Fluid Mech.* **78**, 561–576.

Roberts, B. 1980 Drag and pressure distribution on a family of porous, slotted disks. *J. Aircr.* **17**, 393–401.

Roshko, A. 1954 On the drag and shedding frequency of two-dimensional bluff bodies. *NACA TN* 3169.

Roshko, A. 1961 Experiments on the flow past a circular cylinder at very high Reynolds number. *J. Fluid Mech.* **10**, 345–356.

Roshko, A. 1993 Perspectives on bluff body aerodynamics. *J. Wind Engng Ind. Aerodyn.* **49**, 79–100.

Roshko, A. & Lau, J. C. 1965 Some observation on transition and reattachment of a free shear layer in incompressible flow. In *Proceedings of the Heat Transfer and Fluid Mechanics Institute*, 157.

Saunders, W. S. 1966 Apparatus for reducing linear and lateral wind resistance in a tractor–trailer combination vehicle. *U.S. Patent No.* 3241876.

Schouveiler, L. & Boudaoud, A. 2006 The rolling up of sheets in a steady flow. *J. Fluid Mech.* **563**, 71–80.

Shaw, T. L. 1971 Wake dynamics of two-dimensional structures in confined flows. In *14th Congress of International Association of Hydraulic Research*, vol. 2, Paris, France (see Richter A. & Naudascher E. 1976, *J. Fluid Mech.* **78**, 561–576).

Simmons, J. E. L. 1977. Similarities between two-dimensional and axi-symmetric vortex wakes. *Aeronaut. Q.* **28**, 15–20.

Sumner, D. & Brundrett, E. 1995. Testing three-dimensional bluff-body models in a low-speed two-dimensional adaptive wall test section. *Trans. ASME: J . Fluids Engng* **117**, 546–551.

Tomboulides, A. & Orszag, S. A. 2000 Numerical investigation of transitional and weak turbulent flow past a sphere. *J. Fluid Mech.* **416**, 45–73.

Yeung, W. W. H. 2008 Self-similarity of confined flow past a bluff body. *J. Wind Engng Ind. Aerodyn.* **96**, 369–388.

Yeung, W. W. H. & Parkinson, G. V. 2000. Base pressure prediction in bluff-body potential-flow models. *J. Fluid Mech.* **423**, 381–394.